To appear in the Proceedings of Material Research Society, Spring 2000 Meeting, April 24-28 San Francisco CA.
Symposium AA: Millimeter-Submillimeter Wave Technology, Materials, Devices and Diagnostics, invited paper AA1.6.

MILLIMETER-SUBMILLIMETER VECTOR MEASUREMENTS IN FREE SPACE, AND IN RESONANT STRUCTURES. APPLICATION TO DIELECTRICS CHARACTERIZATION.

Philippe GOY, Michel GROSS, Sylvain CAROOPEN,
AB Millimètre, 52 rue Lhomond, 75005 Paris, France
tel: 33 1 47077100, fax: 33 1 47077071, Email: ~~abmm001@attglobal.net~~
abmillimetre@wanadoo.fr

Juha MALLAT, Jussi TUOVINEN,
Millimetre Wave Laboratory of Finland, Millilab, ESA external laboratory,
Helsinki University of Technology, Radio Laboratory,
P.O. Box 3000, FIN-02015 HUT, Finland,
tel: 358 9 451 2247, fax: 358 9 451 2152, E-mail: juha.mallat@hut.fi

Alain MAESTRINI,
Submillimeter Waves advanced technology group, J.P.L.,
mail stop 168-314, 4800 Oak Grove Drive, 91109-8099 Pasadena CA,
tel: 818 354 5892, fax: 818 393 4683, Email: alain.e.maestrini@jpl.nasa.gov

Guiseppe ANNINO, Maria FITTIPALDI, Massimo MARTINELLI,
Istituto di Fisica Atomica e Molecolare, CNR,
7 Via del Giardino, 56127 Pisa, Italy,
tel: 39 050 3139029, fax: 39 050 3139036, Email: massimo@ifam.pi.cnr.it

I. ABSTRACT.

Usual vector measurements need to compare the signal detected through the Device Under Test DUT, with the signal coming directly from the source. Thanks to a very simple original method developed since 1989, vector detection can also be done with a purely electronic reference. In transmission experiments, there is no need for any directional coupler, and the frequency coverage extends from 8 to 1000 GHz. Quasi-optical propagation is used in the millimeter-submillimeter frequency range. Transmission through dielectric slabs in free space will give an easy measurement of the permittivity. Its real part will be obtained from the phase rotation, and its imaginary part from the amplitude decay. With dielectric coating deposited onto metal, the reflection method is necessary for the characterization. Low-loss materials are characterized with the open cavity perturbation technique. Extremely low loss materials can constitute "whispering gallery" resonators, very easy to excite and characterize.

II. VECTOR MEASUREMENTS WITHOUT DIRECTIONAL COUPLER.

All Vector Network Analyzers VNAs working in the millimeter bands make use of Schottky diode devices as sources (by frequency multiplication, rank N1, from a source S1 at frequency F1, with a phase noise Φ1) and as detectors (by harmonic mixing, rank N2, with a source S2 at frequency F2, with a phase noise Φ2, as Local Oscillator LO). At detection, the IF frequency Fif and the phase noise Φ will be:

$$\text{Fif} = |\text{N1 F1} - \text{N2 F2}| \quad (1)$$
$$\Phi = |\text{N1}\,\Phi 1 - \text{N2}\,\Phi 2| \quad (2).$$

In ordinary VNAs, Fif is tuned at the heterodyne receiver frequency by an appropriate choice of N1 and N2, with N1≠N2, and a precise determination of F1 and F2, involving at least a microwave synthesizer. The phase noise Eq.(2) is eliminated in the heterodyne receiver which must be fed by signals coming from two parallel detection branches (before the DUT, and after). On the contrary, in our VNA [1], there is no need of any microwave synthesizer, the detection LO S2 is PLL-controlled by the source LO S1 (with a frequency offset f in the MHz range), and the harmonic ranks N1 and N2 are the same, so that:

$$N1 = N2 \quad (3),$$
$$F2 = F1 - f \quad (4),$$
$$Fif = N f \quad (5),$$
$$\Phi 1 = \Phi 2 \quad (6),$$
$$\Phi = | N1\,\Phi 1 - N2\,\Phi 2 | = 0 \quad (7).$$

No directional coupler is needed in simple transmission experiments (Fig.1), since the phase reference of the heterodyne receiver can be taken from the quartz reference of the RF synthesizer defining the frequency distance f between F1 and F2 (Eq.4). The noise floor of the heterodyne receiver is low enough to permit detection of microwave signals up to 250 GHz with S1 and S2 being 8-18 GHz centimeter sweepers (using harmonic ranks N up to 15) , and up to 1000 GHz with S1 and S2 being 82-112 GHz widely tunable Gunn oscillators (using harmonic ranks N up to 10). See Fig.2 for the observed dynamic range.

III. FREE SPACE TRANSMISSION.

A very simple quasi-optical bench is made from two lenses placed between emission-detection horns (Fig.3). All samples in this paper were measured at room temperature, but the transmission arrangement can also be used with a cryogenic sample holder [2]. After having recorded the instrumental response, a dielectric plane-parallel sample (thickness e, dielectric constant ε', loss tanδ) can be inserted at the symmetry center S of the setup. The transmission signal will be the sum of a resonant behaviour (the dielectric slab behaving as a Fabry-Pérot resonator), and of an absorption behaviour. Low-loss, high-permittivity samples, like sapphire (ε'=9.4, tanδ=a few 10-4), give a typical resonant response, where the loss is too small to be observed, Fig.4. The permittivity ε', or the refractive index n, can be deduced from the experimental data by looking at the observed phase variation ΔΦ, including an integer number of turns k, and also from the frequency position Fm (m integer) of the maximum transmission, or from the period ΔF between two successive m, m+1 transmission maxima (reflection minima):

$$n = \sqrt{\varepsilon'} \quad (8),$$
$$(n-1)\, e\, F / c = (\Delta\Phi / 360°) + k \quad (9),$$
$$Fm = mc / 2ne \quad (10),$$
$$\Delta F = c / 2ne \quad (11).$$

The amplitude of oscillations can be obtained from the following equations, where the coefficient r is the maximum reflection, obtained at frequencies Fq (q integer), and where t is the corresponding minimum transmission amplitude:

$$Fq = (2q + 1)\, c / 4ne \quad (12),$$

$$r = (\varepsilon' - 1) / (\varepsilon' + 1) \qquad (13),$$
$$r^2 + t^2 = 1 \qquad (14).$$

In the case of a lossy material, the oscillatory behaviour will be hardly visible (Fig.5). The attenuation α, expressed in dB/cm, is easy to measure. The $\tan\delta$ value of the loss is given by:

$$\tan\delta = 1.1\ \alpha(\mathrm{dB/cm}) / n\, F\ (\mathrm{GHz}) \qquad (15).$$

In the case of a sample with intermediate behaviour (Fig.6), the absorption must be taken at the transmission maxima (Eq.10) for measuring the loss.

IV. FREE SPACE REFLECTION.

Reflection measurements performed onto dielectric slabs also give a possible determination of the dielectric constants. The transmission experiments are a little bit more easy (their quality being less dependent on the horn antennas quality), and are generally preferred. However, in the case of a dielectric coating deposited onto a metallic plate, only the reflection measurement is possible. The setup makes use of a directionnal coupler (Fig.7). The dielectric slab acts as a Fabry-Pérot resonator, with a possible interference between the beam reflected from the dielectric surface (Eq.13), and the beam having penetrated into the dielectric (Fig.8), which is totally reflected by the metallic plate. The electric field is damped by a factor p when crossing the dielectric thickness e (i.e. 2e total length):

$$\alpha(\mathrm{dB/cm}) = (10 / 2e\ (\mathrm{mm})) \times 20 \operatorname{Log} p \qquad (16)$$

(Log is with base 10). If the dielectric is lossy ($p<1$), the reflection coming from the rear can be attenuated, so that its amplitude becomes close to the reflection amplitude coming from the front, and thus give visible periodic (Eq.11) minima by interference effects. Sign changes occur in the propagating wave at the front surface (from air to dielectric material), and at the rear surface (from dielectric material to metal), see Fig.8. For this reason, the formula Eq.10 giving the periodic minima, for a dielectric slab in free space, must be replaced here, dielectric slab deposited onto a metallic surface, by:

$$F_m = (2m + 1)\, c / 4n\, e \qquad (17).$$

At resonance (Eq.17), the resulting reflected amplitude is minimum, with a value A, for a unity amplitude of the incident wave, Fig.8. From the observed value A one can deduce the parameter p, then the loss $\tan\delta$ (Eqs.15, 16):

$$A = (p - r) / (1 - rp) \qquad (18),$$
$$p = (A + r) / (1 + rA) \qquad (19).$$

If the thickness e and the loss $\tan\delta$ are small, p is close to unity. Calculations indicate a linear dependence versus frequency F of a(dB), the amplitude A expressed in dB:

$$a(\mathrm{dB}) = 20 \operatorname{Log} A \qquad (20),$$
$$a(\mathrm{dB}) \approx -F\, (n^2\, e \tan\delta / 5.5) \qquad (21).$$

Reflections from a ZrO2 ceramic layer, 0.49 mm thick, deposited onto a stainless steel substrate, present three minimum reflection peaks in the 29-175 GHz interval (Figs.9-10). One observes a -4.63 dB central peak, at 91.2 GHz, which is preferred to the other peaks (at 30.6 and 151.8 GHz), since the horns are better at 91.2 GHz than in the lower, and upper, bands. Eqs.8, 11, 17 give the permittivity $\varepsilon'=26$. Then Eqs.8, 21 give the loss $\tan\delta=0.021$.

V. PERTURBATION OF AN OPEN CAVITY.

The chosen cavity [3] has a nearly semi-spherical geometry. The plane mirror, at bottom, is at a fixed distance D=143.186 mm from the spherical one, at top. It is close to the center of curvature of the spherical mirror, for which R=149.542 mm. The spherical mirror is made of silver coated brass. It includes two coupling holes (for transmission measurements) of 0.8 mm diameter, and 3.5 mm apart, drilled close to the mirror center. The transverse diameter is 180 mm. The plane mirror is made of polished aluminium. It has a diameter of 92 mm. This cavity has the possibility of working in a wide frequency range, from 62 GHz, where Q=138,000, to 665 GHz, where Q=165,000 (Fig.11). The quality factor Q is always higher than 110,000, going over 240,000 in the 90-140 GHz band. Among other advantages (good Q, excellent frequency coverage), the quasi-hemispherical geometry [4] offers a narrow field distribution (waist Wo) located at the center of the plane mirror (Wo=5 mm at 100 GHz). We can therefore characterize samples of small diameters. When varying the frequency, all Fabry-Pérot resonators with a fixed distance L between mirrors give periodic resonances, with an interval ΔF:

$$\Delta F = c / 2L \qquad (22),$$

where c is the speed of light in the medium between mirrors, for instance in air we have measured c=2.99711E8 m/s at 300 GHz. The resonance frequency F of a plane-spherical open cavity is given by:

$$F = \Delta F \, [\, q + 1 + [\, (2p + i + 1)/\pi] \, . \arctan \sqrt{L / (R-L)} \,] \qquad (23),$$

where p, i, q are indexes of the TEMp, i, q mode. The quantity (q+1) is the number of half-wavelengths in the resonator. For fundamental Gaussian modes, p = i = 0, then:

$$F = \Delta F \, (\, q + 1 + 0.4339) \quad \text{with } \Delta F = 1046.58 \text{ MHz} \qquad (24).$$

In a Fabry-Pérot cavity, the wave is reflected many times between mirrors facing each other. The introduction of the dielectric slab between mirrors will create a change of the resonant frequency (change of the electrical dimensions of the cavity), which will give the permittivity ε', and a damping of the resonance (decrease of the quality factor due to the losses inside the sample) which will give a measurement of $\tan\delta$ (Fig.12). With open cavities offering empty quality factors Qo above 10+5, the determination of losses $\tan\delta$>10-4 is possible. For the best matching of the wave at the surface of the sample, measurements must be done at frequencies for which the number of half-wavelengths inside the sample is as close as possible to an integer. The characterization of a dielectric material will be done at one of these frequencies Fs with the sample inside the cavity. The loaded quality factor Qs will also be measured. Then the sample is removed, without any change of the distance D between mirrors. The empty cavity gives a resonance frequency Fo and a quality factor Qo. From the four parameters Fs, Qs, Fo, Qo and from the geometry of the cavity and of the sample, one can calculate the permittivity ε' and the loss $\tan\delta$ of the sample. For that purpose, there are iterative equations [3] which are included in the software of the vector analyzer.

The best measured low-loss polymer is HDPE (High-Density-Poly-Ethylen) where the results on four samples, from 90 to 310 GHz, are ε'=2.323+/-0.016, $\tan\delta$=(2.45+/-0.15)10-4. With three samples of Teflon in the 84-94 GHz interval, the results are ε'=2.040+/-0.007, $\tan\delta$

=(3.1+/-0.3)10-4, and, in the interval 251-305 GHz: 2.033+/-0.01, and tanδ=(4.5+/-0.3)10-4. At 665 GHz, the loss in Teflon is tanδ=(12+/-1)10-4, Fig.13. Rexolite (one sample) gives at 95 GHz: ε'=2.535, tanδ=13.2 10-4, and at 257 GHz: ε'=2.527, tanδ=27 10-4.

VI. WHISPERING GALLERY RESONATORS.

The open cavity perturbation technique, as described above (section V), presents sensitivity limitations for characterizing very low-loss materials (practically below 10-4). If the dielectric material constitutes the resonator itself, there is no limitation. Very good whispering gallery resonators can be made from low-loss dielectric materials, in a sphere or disk shape. The wave is coupled into the dielectric material by an evanescent wave emitted from a total reflection prism, or from cone-shaped dielectric waveguides (Fig.14). The resonant modes correspond to an integer number of wavelengths along the diameter D, with a frequency interval ΔF close to:

$$\Delta F \approx c / \pi n D \quad (25),$$

see for instance Fig.15 in the case of a cristalline quartz resonator, 18mm diameter, 1mm thick, giving resonances every 2.3 GHz. As soon as the chosen resonance mode is at a frequency high enough so that diffraction is negligible (Fig.16), and also when the coupling of the whispering cavity mode is weak enough to avoid the damping of the quality factor, one observes the intrinsic quality factor Qo, which is related to the dielectric loss by the simple relationship:

$$Qo = 1 / \tan\delta \quad (26).$$

A 15mm diameter, 0.6mm thick PolyEthylen resonator will give Qo=2400 at 572 GHz, corresponding to tanδ=4.2 10-4. In a 18mm diameter, 1mm thick cristalline quartz disk, one finds Qo=29740 and 23390 at 108 and 383 GHz, respectively. One also finds Qo=12000 and 11280 at 665 and 761 GHz, respectively (Figs.17-22). In crystals, one must observe an inverse Qo dependence versus frequency F:

$$F\,Qo = \text{constant} \quad (27).$$

In the case of the quartz disk of Figs.15-22, Eq.27 gives, at frequencies 383, 665 and 761 GHz, an average F Qo = 8.5 10+6 GHz, which is an extremely good figure. It means that the tanδ values are 4.5, 6.65, 8.95 10-5, at respective, increasing, frequencies. At 108 GHz, the observed value F Qo = 3.2 10+6 GHz is lower. When looking closely at the resonances shown Fig.15, one observes that the resonances at the lower frequencies (below 86 GHz) are clearly damped by diffraction losses. Even the resonances labelled 1-2-3-4 (Figs.15-16), at higher frequencies (up to 108 GHz), have quality factors 2400, 5000, 8200, 15400 (respectively) increasing with frequency, which shows that they are still diffraction limited. From Eq.27 the intrinsic loss in this quartz sample must be, at 108 GHz, as low as tanδ=1.27 10-5. This seems to be one of the lowest losses ever measured at room temperature.

AKNOWLEDGEMENTS.

This work has been partially supported by the European contract N° ERBFMGECT950008 "Umbella", February 1996-February 2000.

REFERENCES.
[1] French Patent CNRS-ENS 1989, extended by AB MILLIMETRE to Europe, Japan and the USA: US Patent N° 5 119 035 (June 2, 1992).
[2] J.A. Reedijk, H.C.F. Martens, B.J. Smits, H. Brom, Review of Scientific Instruments, **71,** 478 (2000).
[3] T.M. Hirvonen, P. Vainikainen, A. Lozowski, A. Räisäinen, IEEE Transactions on Instrumentation and Measurements, **45,** N°4, 780 (1996).
[4] R. Heidinger, F. Königer, 14th Int. Conf. on IR and mm Waves, Würzburg, 2-6 octobre 1989, p.541, M. Von Ortenberg Ed. (1989).

Fig.1.
Transmission setup. Below 250 GHz, the local oscillators S1 and S2 are 8-18 GHz centimeter sweepers. The Schottky multiplier (at left) and harmonic mixer (at right) work with harmonics up to 15. Above 250 GHz S1 and S2 are 82-112 GHz Gunn oscillators. The Schottky multiplier (at left) and harmonic mixer (at right) work with harmonics up to 10. Then, with these two Gunn extensions, the isolators are replaced by high-pass filters.

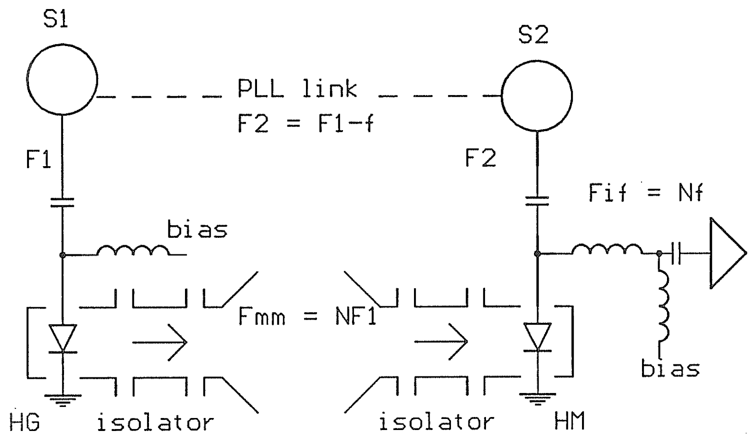

Fig.2.
Dynamic range observed versus frequency. Branch a) without Gunn extensions. Branch b) with one Gunn extension. Branch c) with two Gunn extensions.

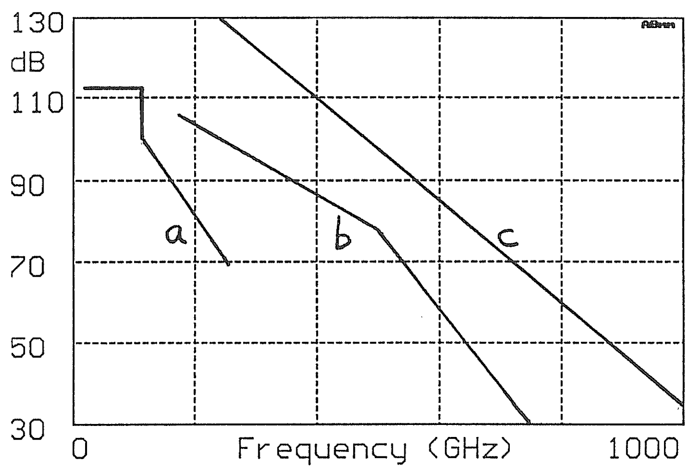

Fig.3.
Free-space transmission setup. With Gunn extensions, the isolators are replaced by high-pass filters, sometimes cascaded with attenuators (in order to reduce the standing waves).

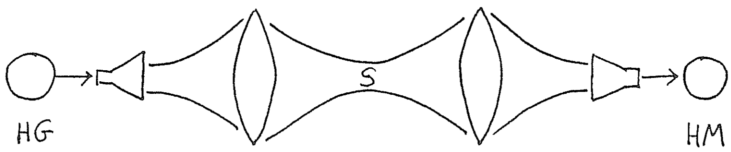

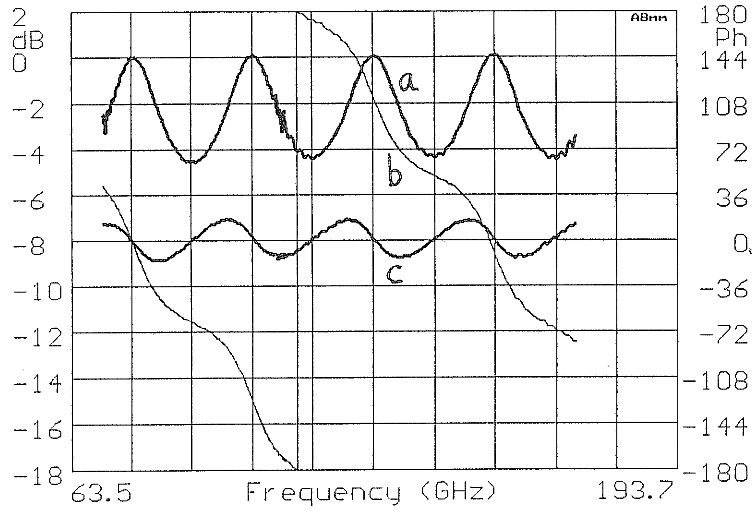

Fig.4.
Transmission through a 1.91mm thick sapphire slab. In a) amplitude in dB, in b) actual phase in Degrees, in c) phase without its linear frequency dependence (Eqs.8-9 give n=3.062, ε'=9.38). The refractive index n determination from the phase measurement will be exact for maximum, and minimum, transmission. The amplitude maxima are close to zero, therefore it is only possible to give an upper limit: tanδ<10-3.

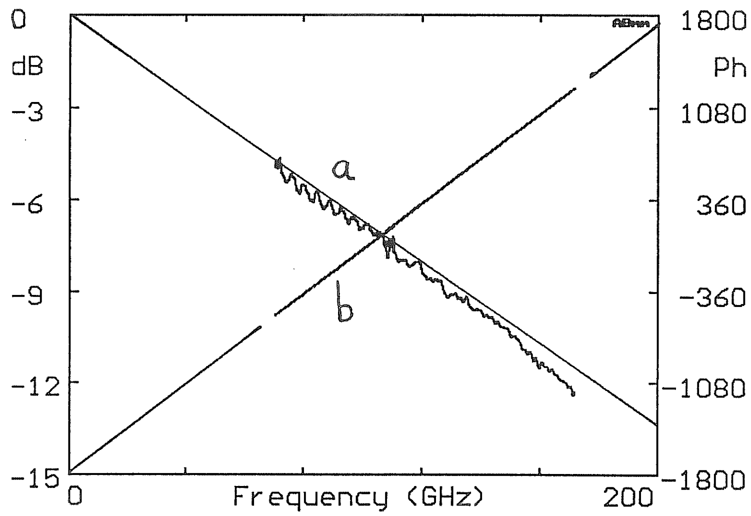

Fig.5.
Transmission through a 21mm thick Araldite (Epoxy) slab. In a) amplitude. In b) phase (taken with an opposite sign for clarity), which is extremely linear, and in good alignment with the origin: the n value does not change in the 0-170 GHz interval, n=1.701, ε'=2.894. On a), one sees a large attenuation, and a small resonant contribution. The absorption remains constant up to ca 150 GHz. Eq.15 gives: tanδ=0.021. Above 150 GHz, the loss increases very rapidly, giving 0.026, 0.031, 0.036, 0.037, 0.041 at 285, 380, 475, 570, 665 GHz, respectively. At all these frequencies, n and ε' do not change significantly.

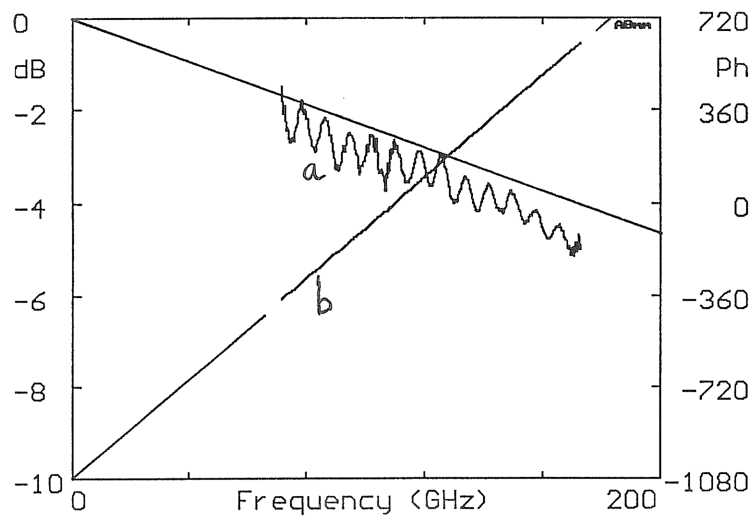

Fig.6.
Transmission through a 10.9mm Nylon slab. Like in Fig.5, with a smaller loss, giving a more visible oscillatory behaviour. The linear phase variation gives a constant refractive index in the 0-170 GHz interval n=1.75, ε'=3.07. Below 120 GHz the loss is tanδ=0.014. Similarly to Fig.5, at the same frequencies, loss is 0.020, 0.026, 0.032, 0.037, 0.042.

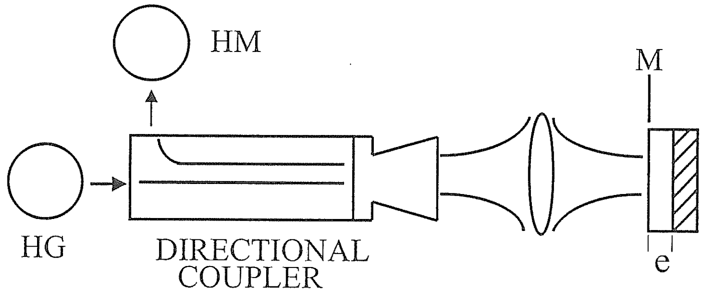

Fig.7.
Experimental setup for observing reflection from a dielectric slab. The calibration is made with a metallic mirror placed at M.

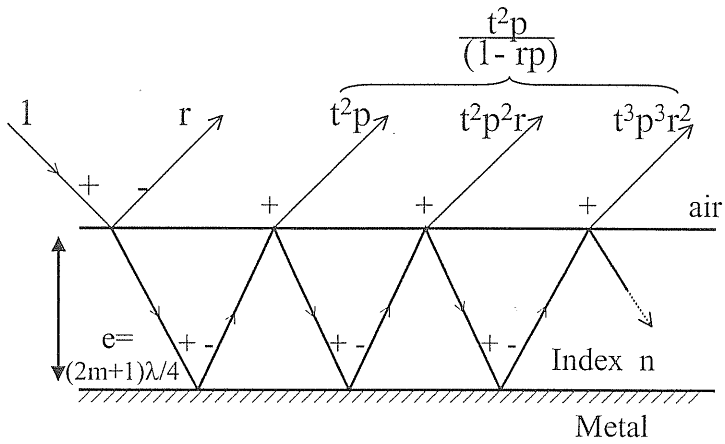

Fig.8.
Construction of the interference pattern at reflection onto the dielectric material of thickness e, index n and loss tanδ. The incident beam, represented with an angle from the direction perpendicular to the dielectric slab for clarity, has an electrical field amplitude 1. It is reflected at the air/dielectric interface with an amplitude r (Eq.13) and a change of sign. The beam which has penetrated into the dielectric material gives a series of contributions. The reflection dielectric/metal makes also a change of sign. The resonance condition (minimum reflection) is that the optical slab thickness n e is an odd multiple of λ/4, see Eq.17.

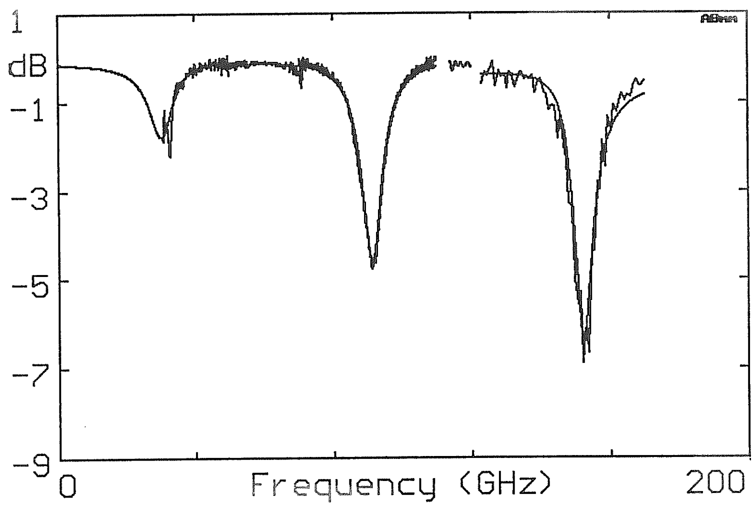

Fig.9.
Amplitude reflection from a ZrO2 ceramics deposited onto stainless steel, thickness e=0.49mm. A Lorentzian fit has been made at each resonance. The positions of the resonances (Eq.17) give:
n=5.1, ε'=26. The amplitude of the peak at 91.2 GHz gives (Eq.21): tanδ=0.021.

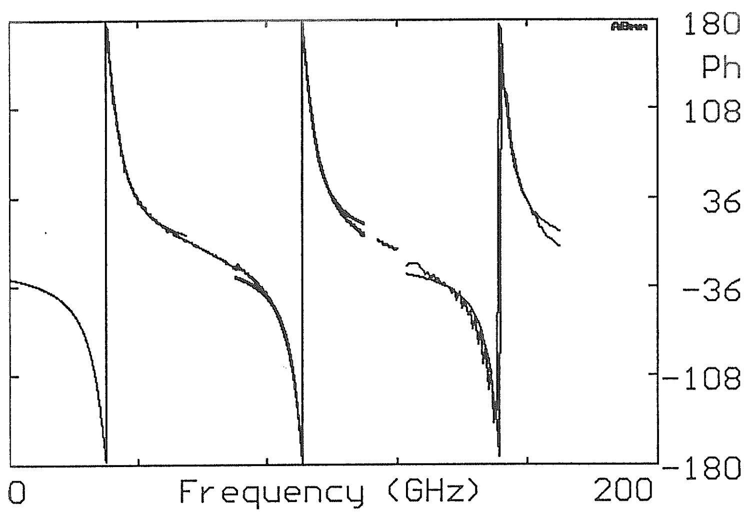

Fig.10.
Phase variations (and local Lorentzian fits) observed together with Fig.9. If the dielectric presents a negligible loss (p=1), no resonance could be visible on the amplitude (Fig.9). On the contrary the phase would give the same large variations.

Fig.11.
Transmission across the empty Fabry-Pérot resonator described in section V. Experimental traces and Lorentzian fit, a) amplitude, b) phase. The quality factor is excellent: Q=165000. The vertical scale is with 0dB at the noise floor.

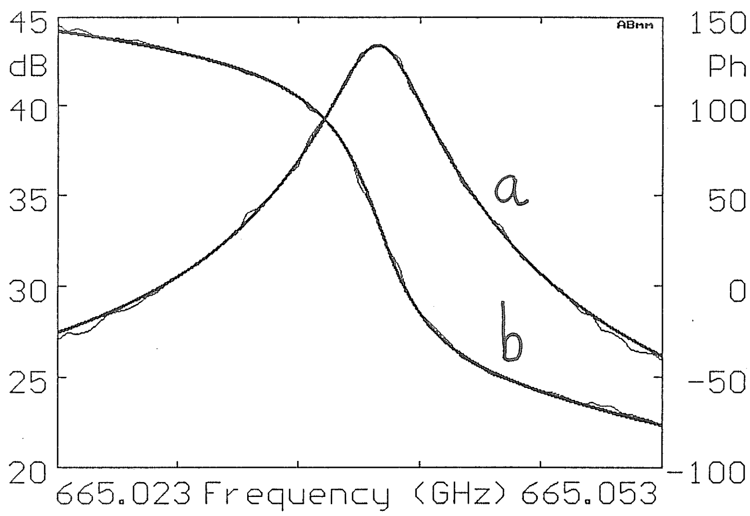

Fig.12.
Like in Fig.11. Transmission across the Fabry-Pérot resonator. At right, it is empty: Fo=251.6329 GHz, Qo=139850. At left, the cavity is loaded with a 10mm thick Teflon sample. The resonance frequency is Fs=251.3955 GHz and the loaded quality factor is Qs=25030. Calculations give:
ε'=2.042 and tanδ=0.00046.

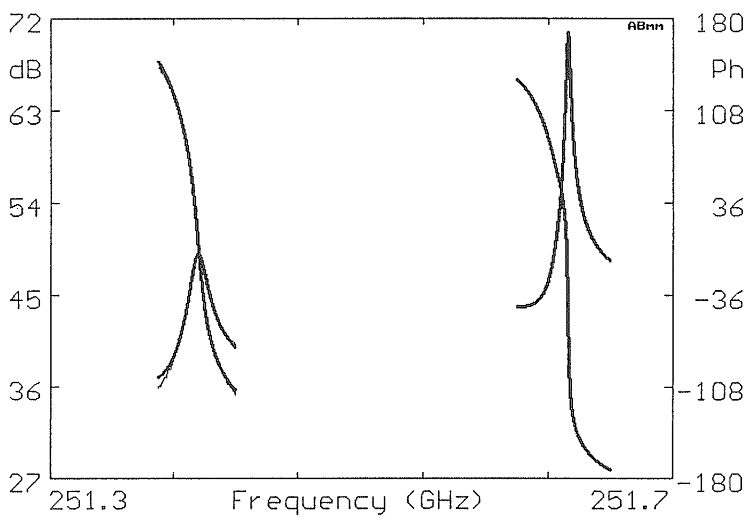

Fig.13.
The upper trace (shifted upwards for clarity) shows the transmission across the empty Fabry-Pérot resonator. Due to the very high frequencies and to the large size of the cavity, many modes are visible, even with a diaphragm of 12mm placed on the plane mirror. The q=634, p=i=0 mode, with its Lorentzian fit, is shown by an arrow (local sweep already shown Fig.11).
The lower trace (shifted downwards for clarity) shows the transmission across the same Fabry-Pérot resonator loaded with a 10.03mm thick Teflon sample. The diffraction losses cause all resonance peaks to disappear, but not the main modes p=i=0, shown with their Lorentzian fits. The quality factor is Qs=10950. Calulations give:
ε'=2.065 and tanδ=0.0012.

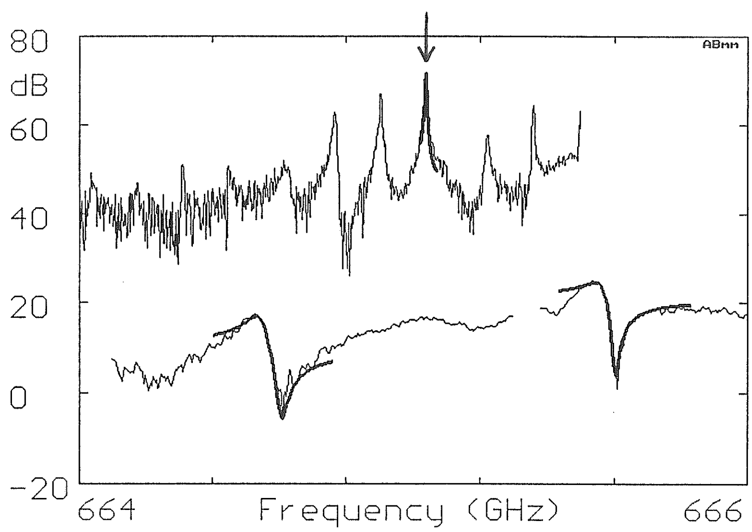

Fig.14.
Coupling of a submillimeter wave into the dielectric disk resonator, in order to create whispering gallery modes. The dielectric waveguides were made by a glass-blower from cylindrical rods of fused silica. Their large diameter is a few millimeters. Their tip has capillary dimensions. Their opposite ends are also cone-shaped. They pick-up the wave at the empty cylindrical end of metallic pyramidal transitions, connected to the microwave source and detector through very small rectangular waveguides. The coupling and adjustments (over-coupling, critical coupling, under-coupling) are very easy.

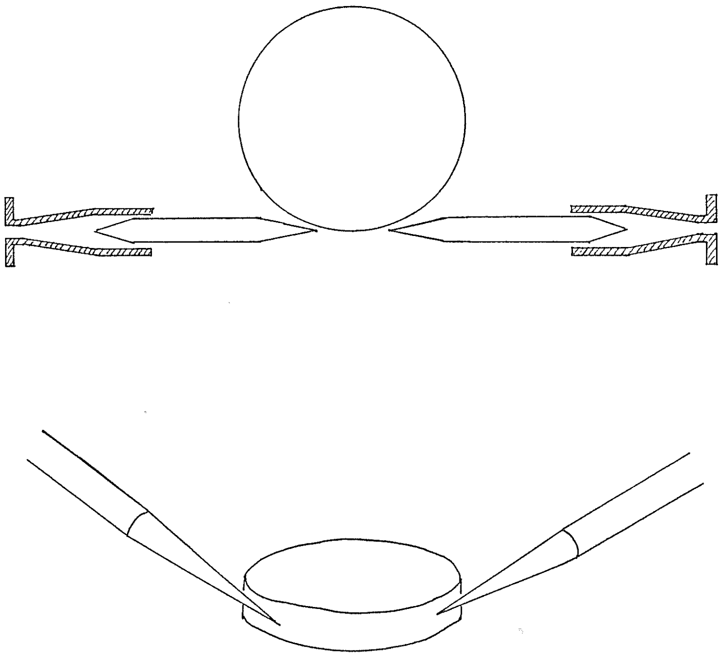

Fig.15.
Whispering gallery resonances observed in a 18mm diameter, 1mm thick, cristalline quartz disk. The low frequency edge is clearly diffraction-limited (the size of the sample is not large enough for the largest wavelengths).

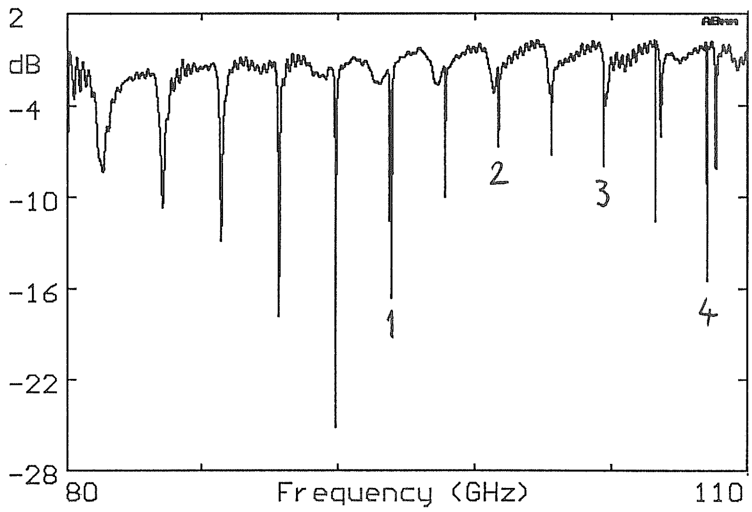

Fig.16.
Polar plot of the resonances labelled 1-2-3-4 in Fig.15. The sweep has been operated with a constant frequency step of 5 MHz. The peak 1 appears as a circle, since it contains many steps: its quality factor is low Q=2400. The peaks 2-3 are polygons (Q=5000 and Q=8200), the peak 4 is a sharp triangle (Q=15400). This rapid Q evolution with frequency shows that the upper frequency resonance (peak 4) at 108 GHz is still diffraction-limited and cannot give, even when very much undercoupled, the intrinsic loss value $\tan\delta$ of the quartz.

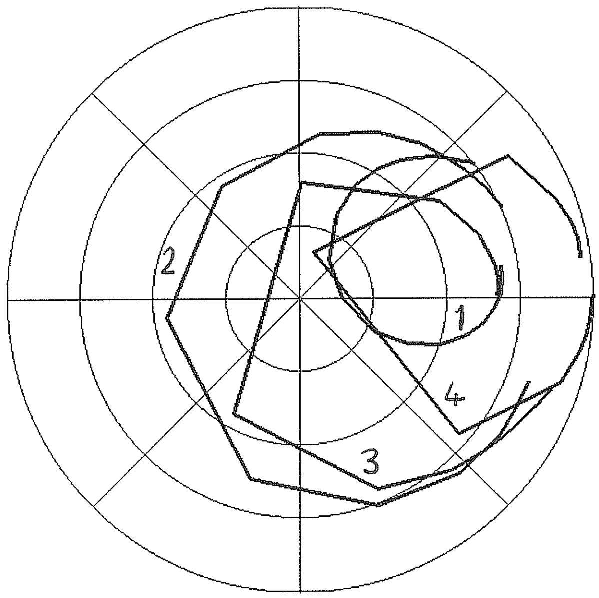

Fig.17.
Resonances in the 18mm diameter, 1mm thick cristalline quartz resonator, observed on the amplitude with a decreasing coupling from a) to d). Experimental traces and Lorentzian fits. In a) the minimum amplitude is very deep, which is typical at the critical coupling.

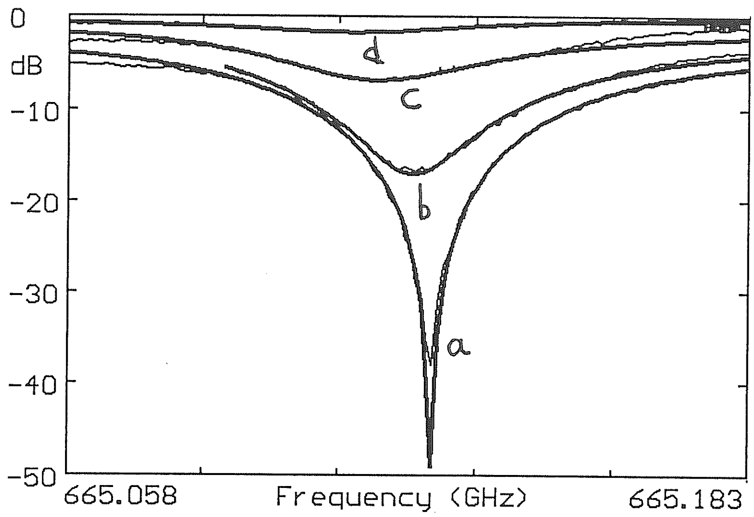

Fig.18.
Same as Fig.17, phase variation. In a) the step in phase is 180°, which is typical for a critical coupling.

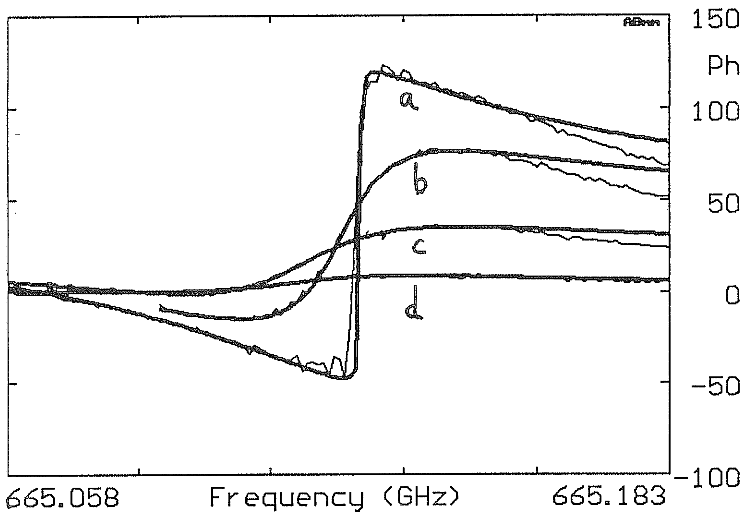

Fig.19.
Polar plots corresponding to Figs.17-18. In a) the origin belongs to the circle of resonance, which is typical for a critical coupling. From a) to d), the obtained quality factors are Q = 6520, 6910, 9660, and 11970, the last value being viewed as the intrinsic quality factor, since it appears very much undercoupled (small circle, far from the origin).

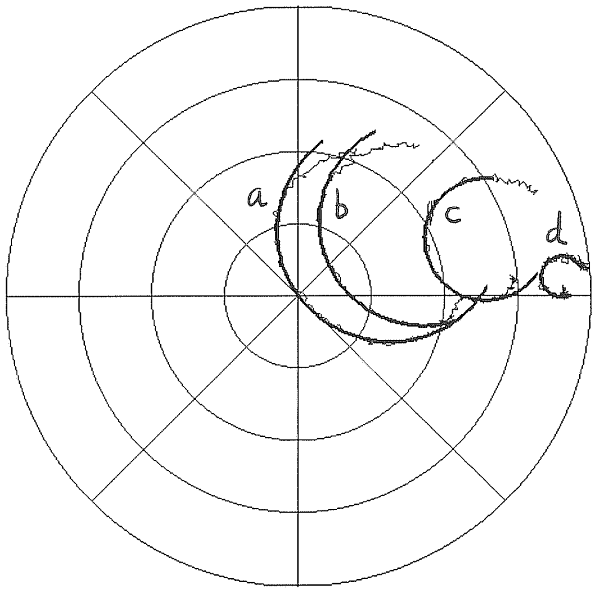

Fig.20.
Resonances in the 18mm diameter, 1mm thick cristalline quartz resonator, observed on the amplitude with a decreasing coupling from a) to b). Experimental traces and Lorentzian fits. In a), the minimum amplitude is very deep, which is typical at the critical coupling.

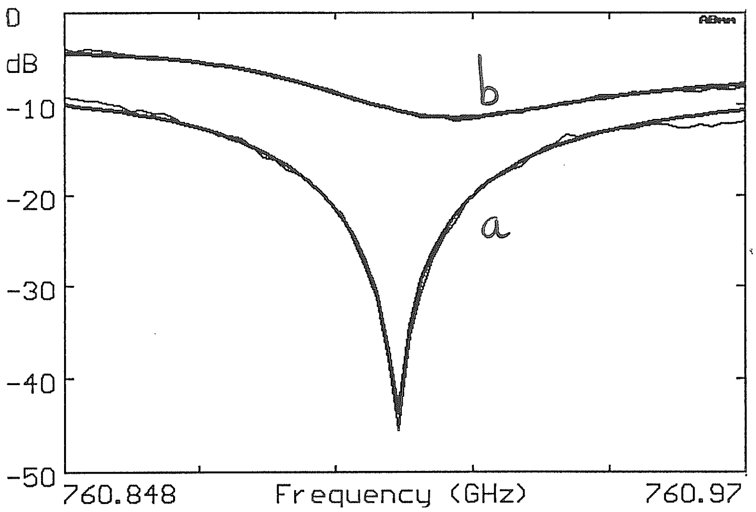

Fig.21.
Same as Fig.20, phase variation. In a) the step in phase is 180°, which is typical for a critical coupling.

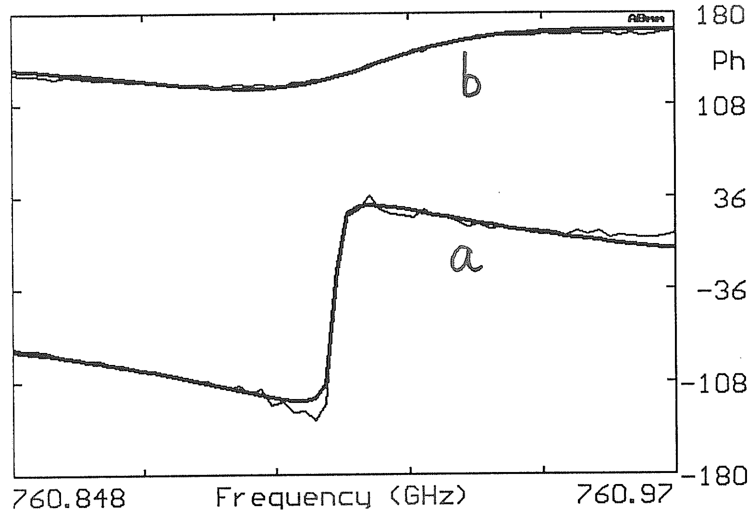

Fig.22.
Polar plots corresponding to Figs.20-21. In a), the origin belongs to the circle of resonance, which is typical for a critical coupling. From a) to b), the obtained quality factors are Q = 7500 and 9160, the last value is not viewed as the intrinsic quality factor, since it appears not enough undercoupled. Size and position of circle b) can be compared to the circle c) in Fig.19, which had a Q=9660 instead of the intrinsic 665 GHz value Q=11970. Extrapolating from these values, the intrinsic value here at 761 GHz must rather be Q=11350.